Electronic Supplementary Material (ESI) for Dalton Transactions.

Supporting Information

(FeMnCe)-co-doped MOF-74 with significantly improved performance for overall water splitting

Ning Chai [a], Yuxuan Kong [a], Tian Liu [a], Shuanglu Ying [a], Qiao Jiang [a], and Fei-Yan Yi*[a, b]

[a] School of Materials Science and Chemical Engineering, Ningbo University, Ningbo, Zhejiang, 315211, P. R. China, E-mail: yifeiyan@nbu.edu.cn

[b] Key Laboratory of Photoelectric Detection Materials and Devices of Zhejiang Province, Ningbo, 315211, P. R. China.

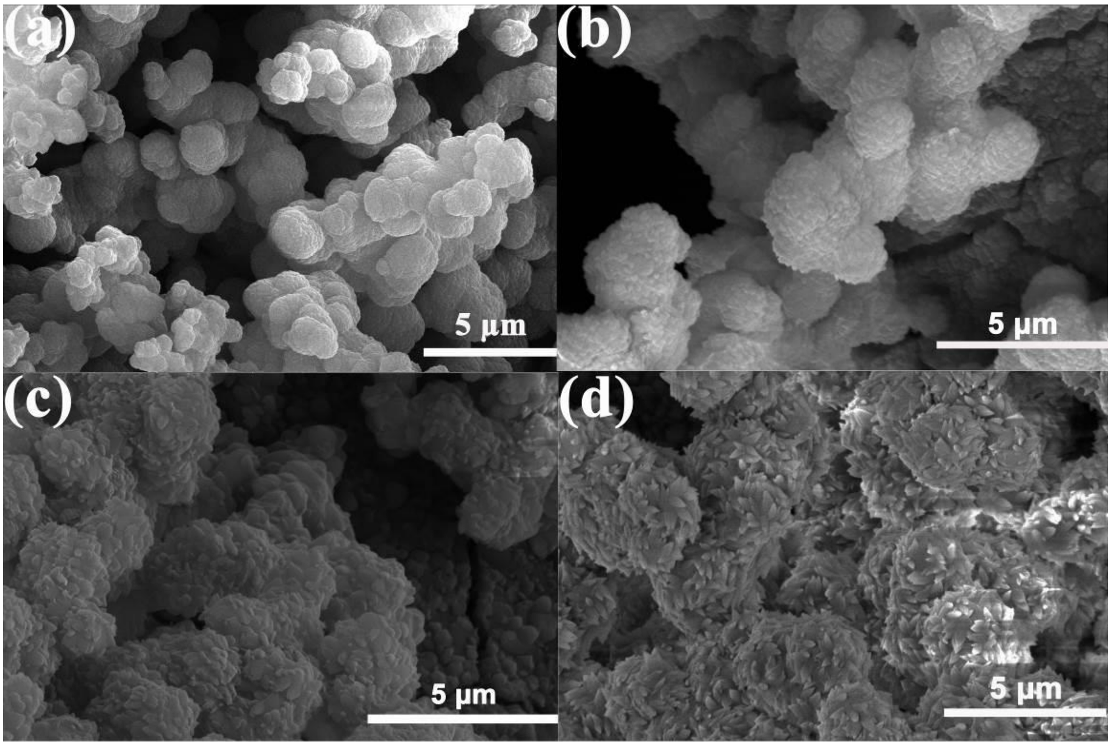

Fig. S1 SEM of (a)Fe-MOF-74/NF, (b)$FeCe_{0.5}$-MOF-74/NF, (c)$FeCe_1$-MOF-74/NF, (d)$FeCe_2$-MOF-74/NF

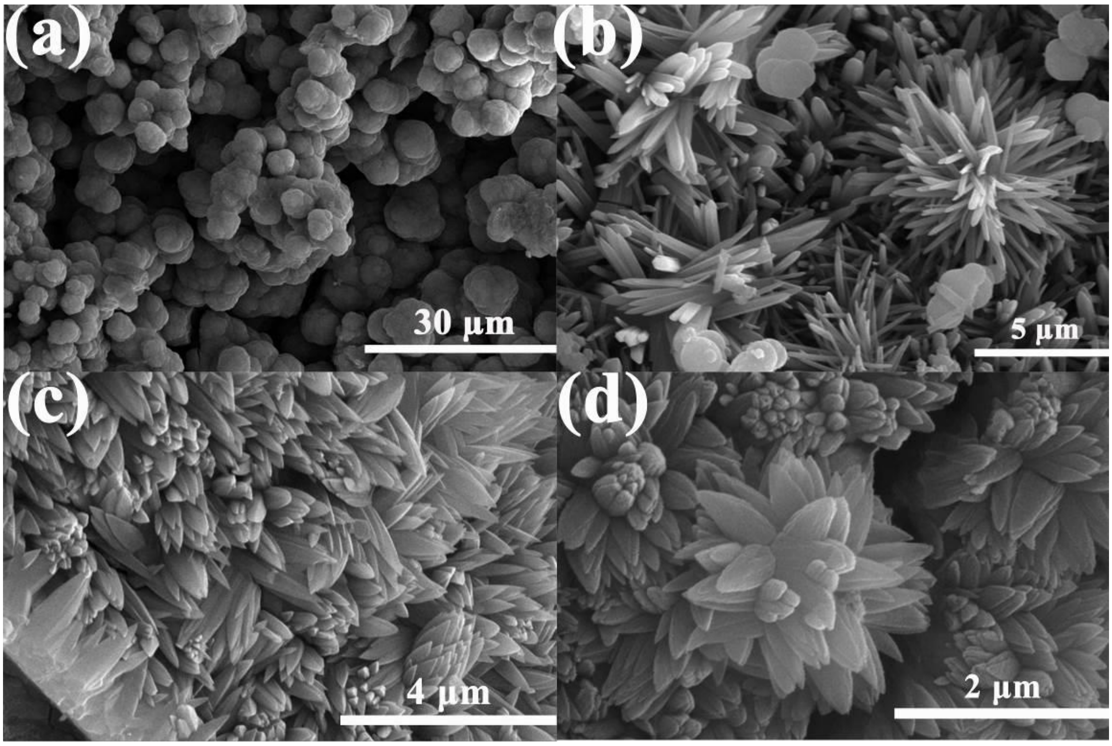

Fig. S2 SEM of (a)Mn-MOF-74/NF, (b)$Mn_6Ce_{0.5}$-MOF-74/NF, (c)Mn_6Ce_1-MOF-74/NF, (d)Mn_6Ce_2-MOF-74/NF

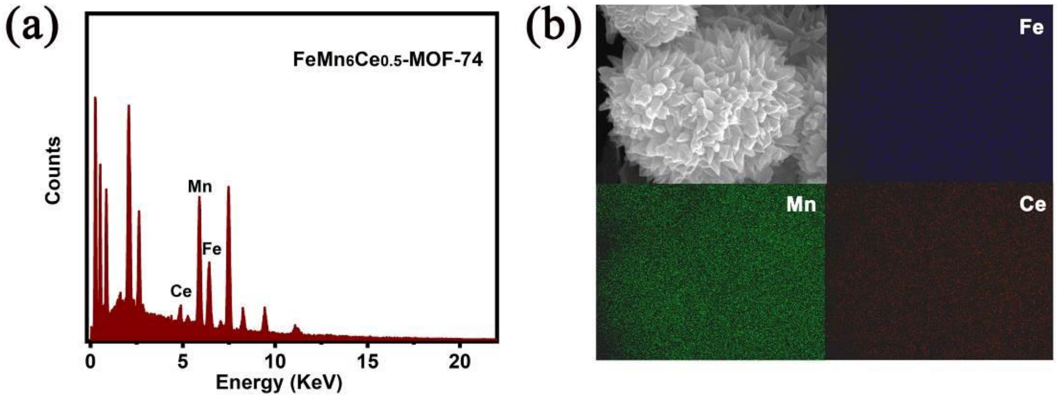

Fig. S3 (a) EDX patterns of $FeMn_6Ce_{0.5}$-MOF-74/NF; (b) elemental mapping of $FeMn_6Ce_{0.5}$-MOF-74/NF

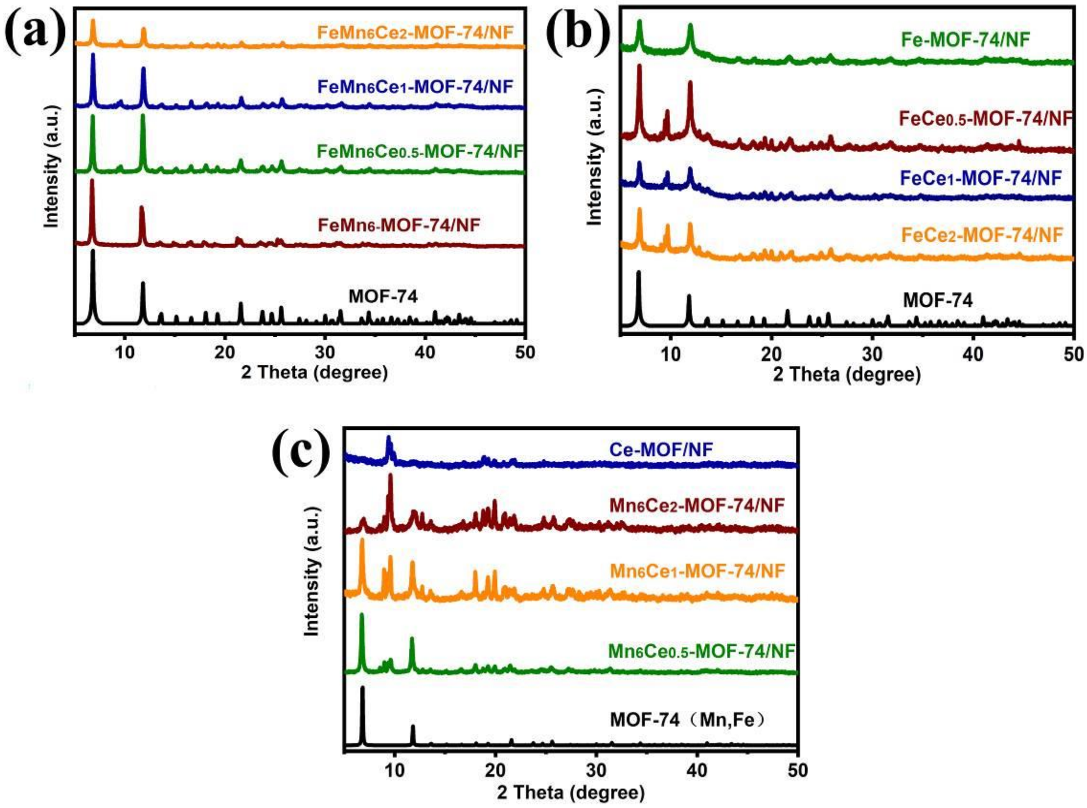

Fig. S4 XRD patterns of (a) (FeMnCe)-MOF-74 series; (b) FeCe-MOF-74 series and (c) MnCe-MOF-74 series.

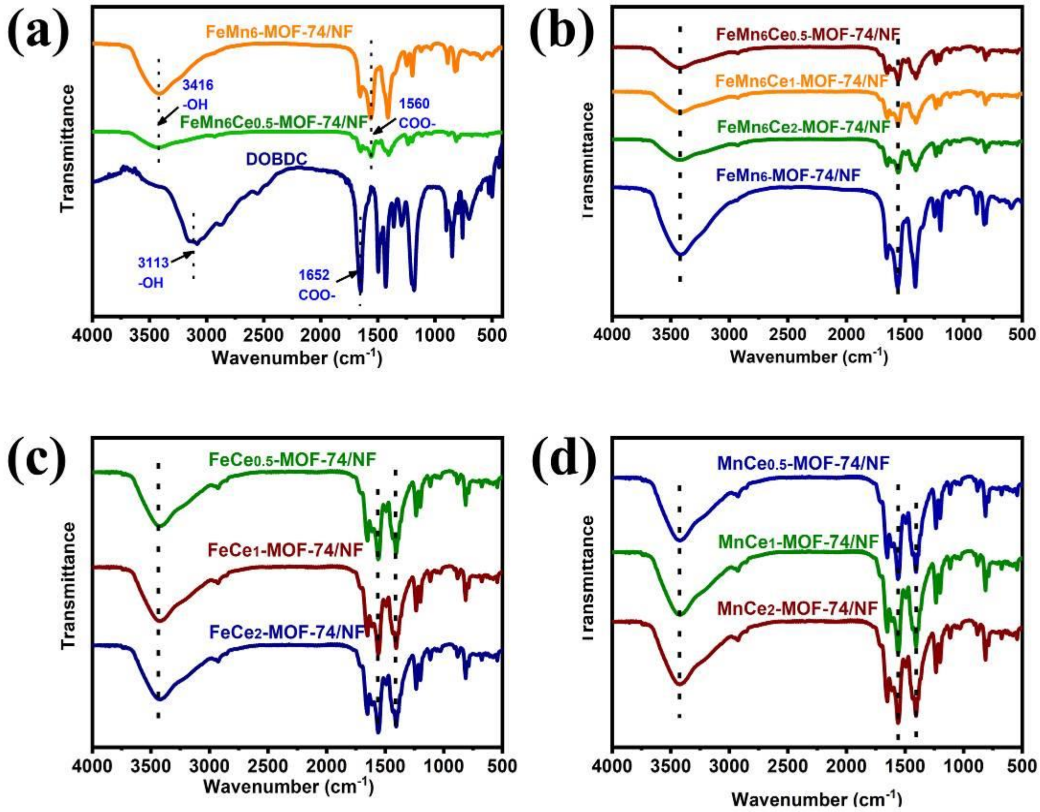

Fig. S5 FT-IR patterns of (a) $FeMn_6$-MOF-74/NF, $FeMn_6Ce_{0.5}$-MOF-74/NF, and ligand DOBDC; (b) (FeMnCe)-MOF-74 series; (c) FeCe-MOF-74 series and (d) MnCe-MOF-74 series.

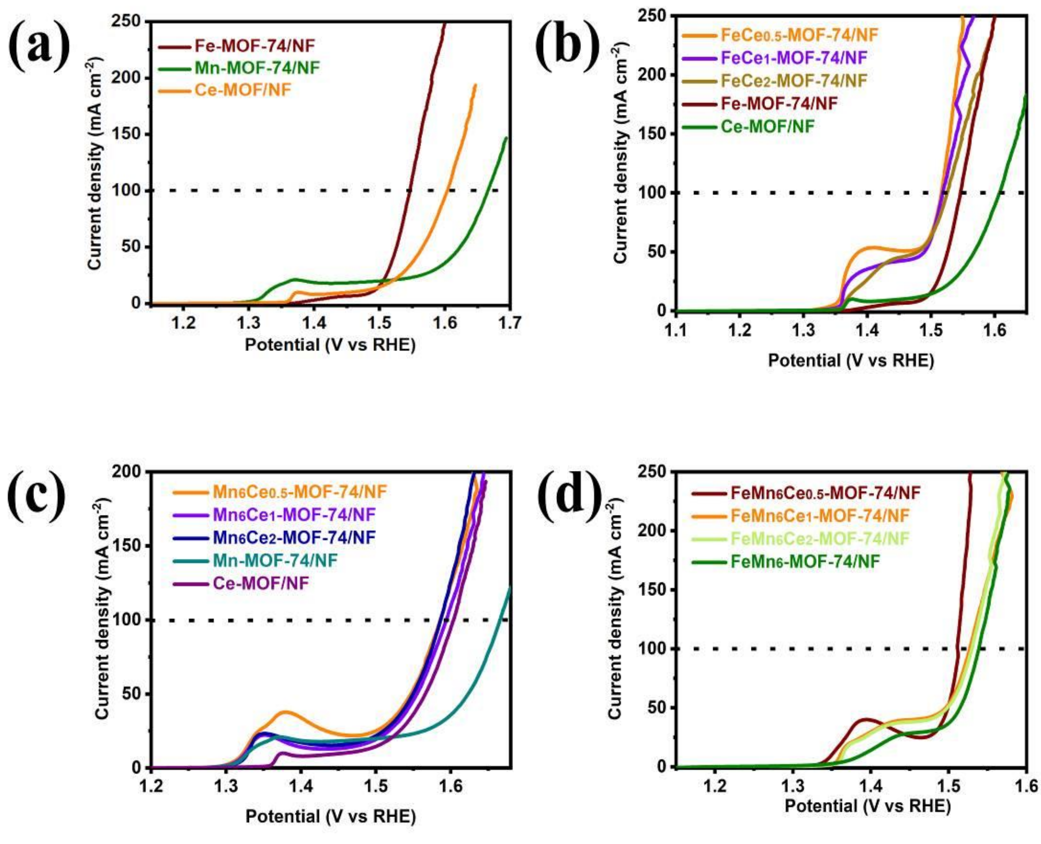

Fig. S6 OER performances of all as-prepared materials in 1 M KOH. The LSV plots of (a) single metal-MOF-74; (b) FeCe-MOF-74 series; (c) MnCe-MOF-74 series and (d) (FeMnCe)-MOF-74 series.

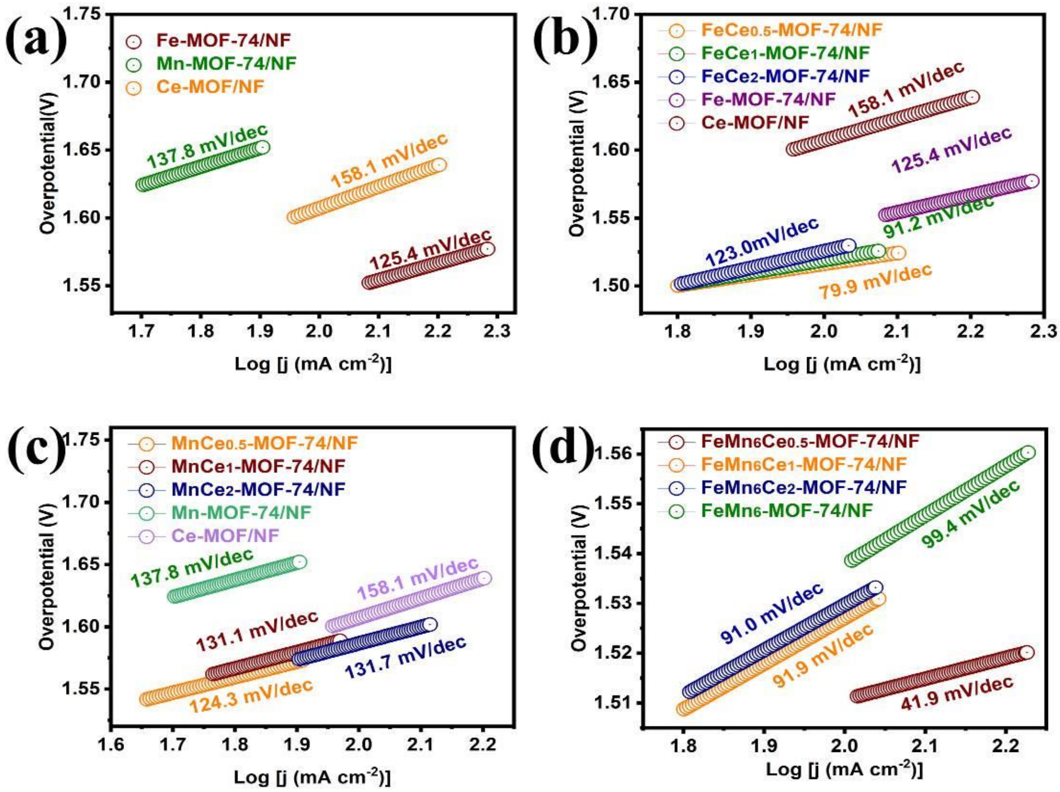

Fig. S7 OER performances of all as-prepared materials in 1 M KOH. Tafel plots of (a) single metal-MOF-74; (b) FeCe-MOF-74 series; (c) MnCe-MOF-74 series and (d) (FeMnCe)-MOF-74 series.

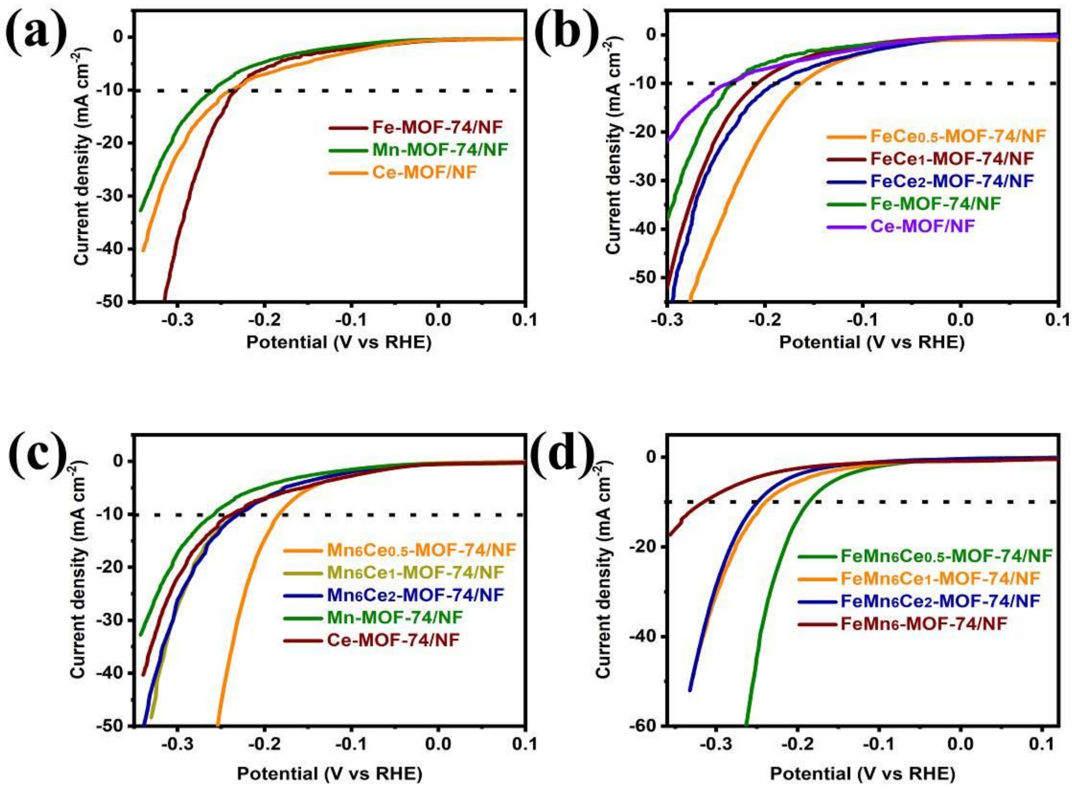

Fig. S8 HER performances of all as-prepared materials in 1 M KOH. The LSV plots of (a) single metal-MOF-74; (b) FeCe-MOF-74 series; (c) MnCe-MOF-74 series and (d) (FeMnCe)-MOF-74 series.

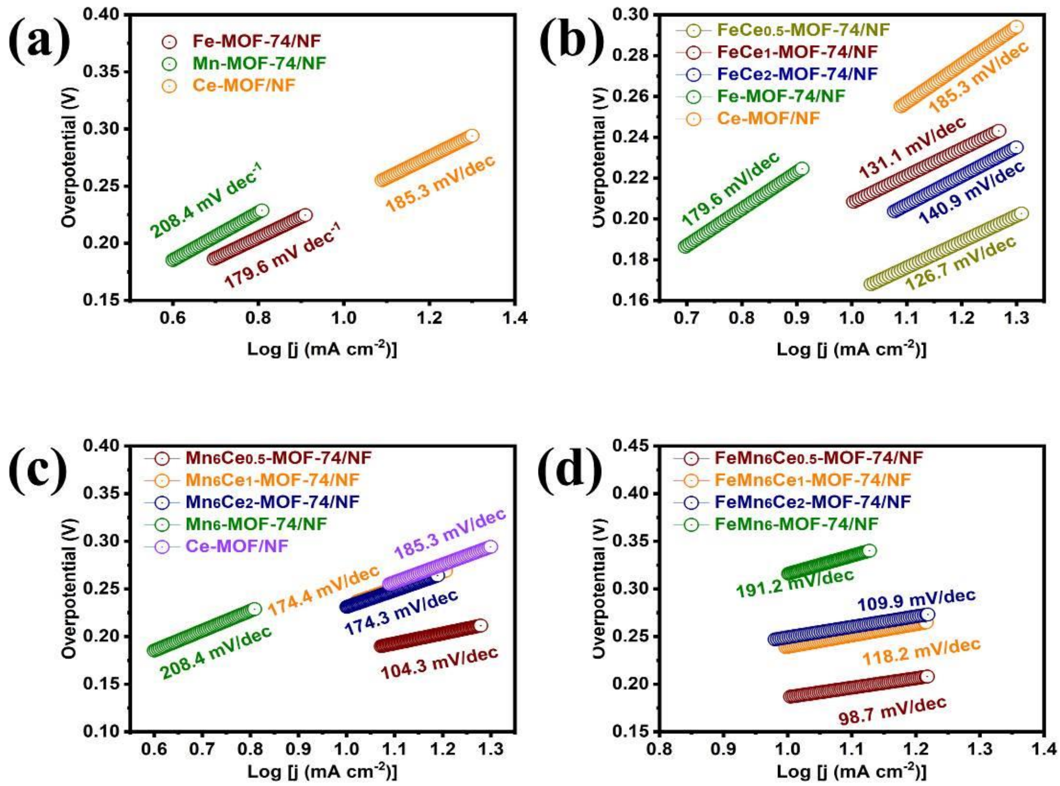

Fig. S9 HER performances of all as-prepared materials in 1 M KOH. Tafel plots of (a) single metal-MOF-74; (b) FeCe-MOF-74 series; (c) MnCe-MOF-74 series and (d) (FeMnCe)-MOF-74 series.

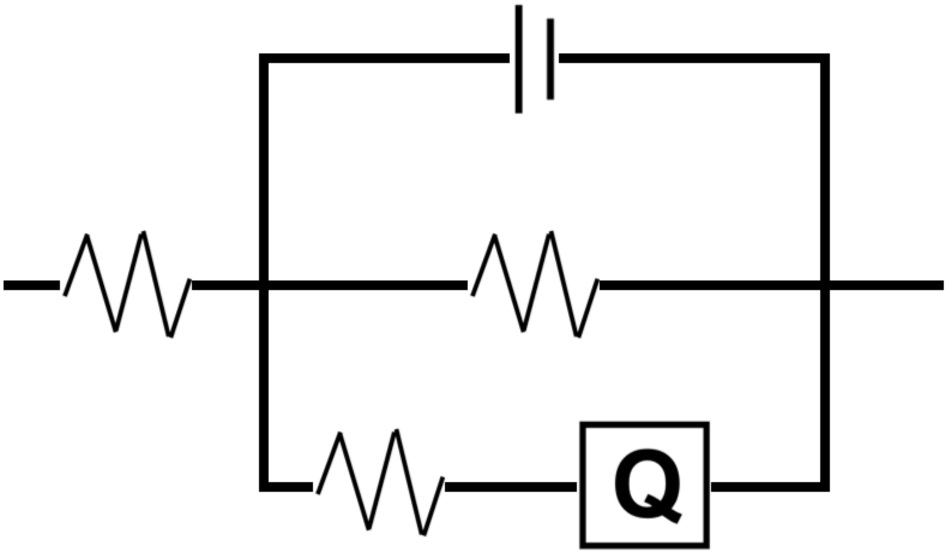

Fig. S10 The equivalent circuit model for electrochemical impedance tests.

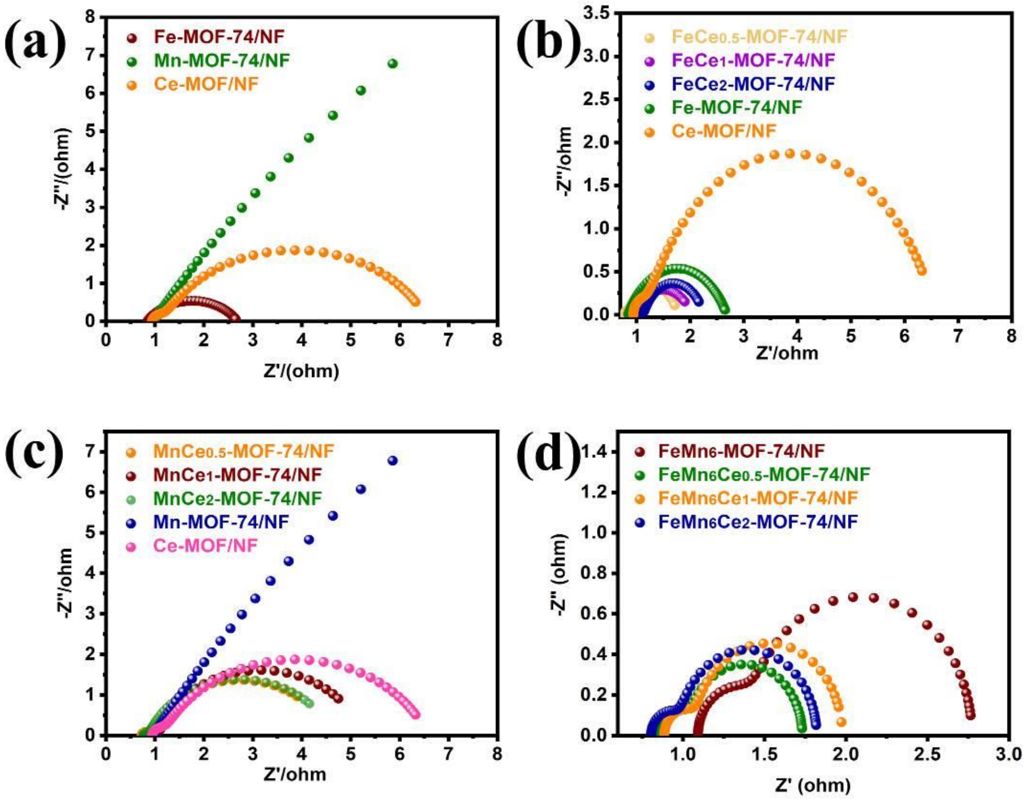

Fig. S11 OER performances of all as-prepared materials in 1 M KOH. Nyquist plots of (a) single metal-MOF-74; (b) FeCe-MOF-74 series; (c) MnCe-MOF-74 series and (d) (FeMnCe)-MOF-74 series.

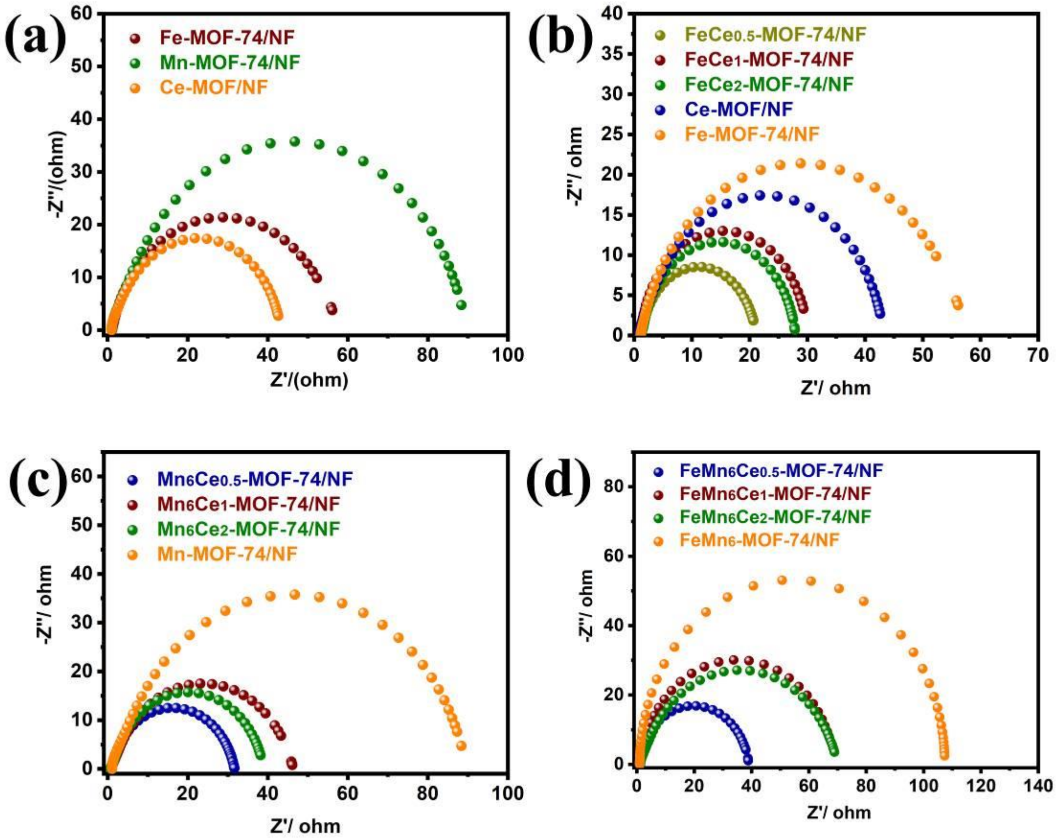

Fig. S12 HER performances of all as-prepared materials in 1 M KOH. Nyquist plots of (a) single metal-MOF-74; (b) FeCe-MOF-74 series; (c) MnCe-MOF-74 series and (d) (FeMnCe)-MOF-74 series.

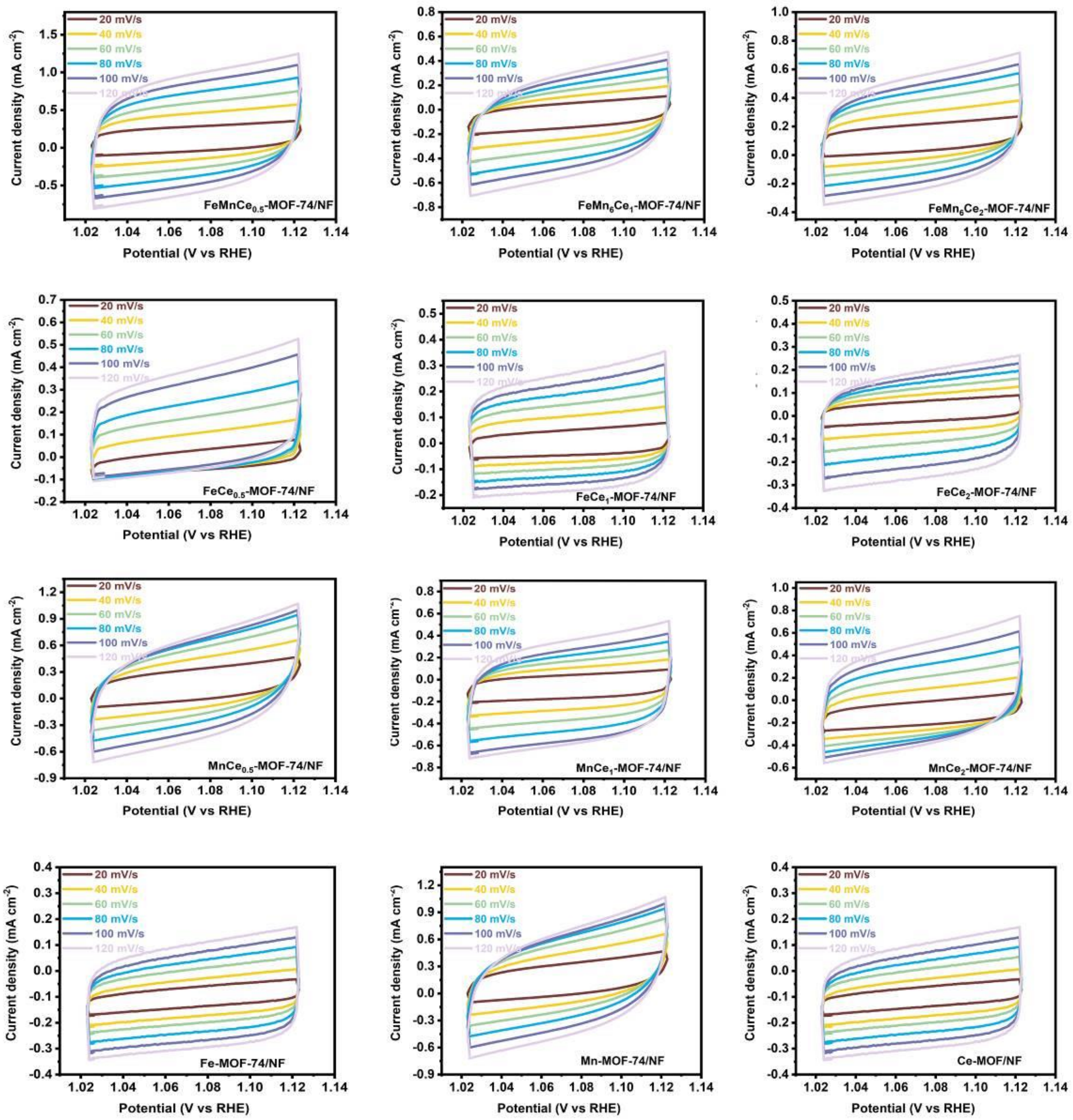

Fig. S13 CV curves of all as-prepared materials at scan rates ranging from 20 to 120 mV/s

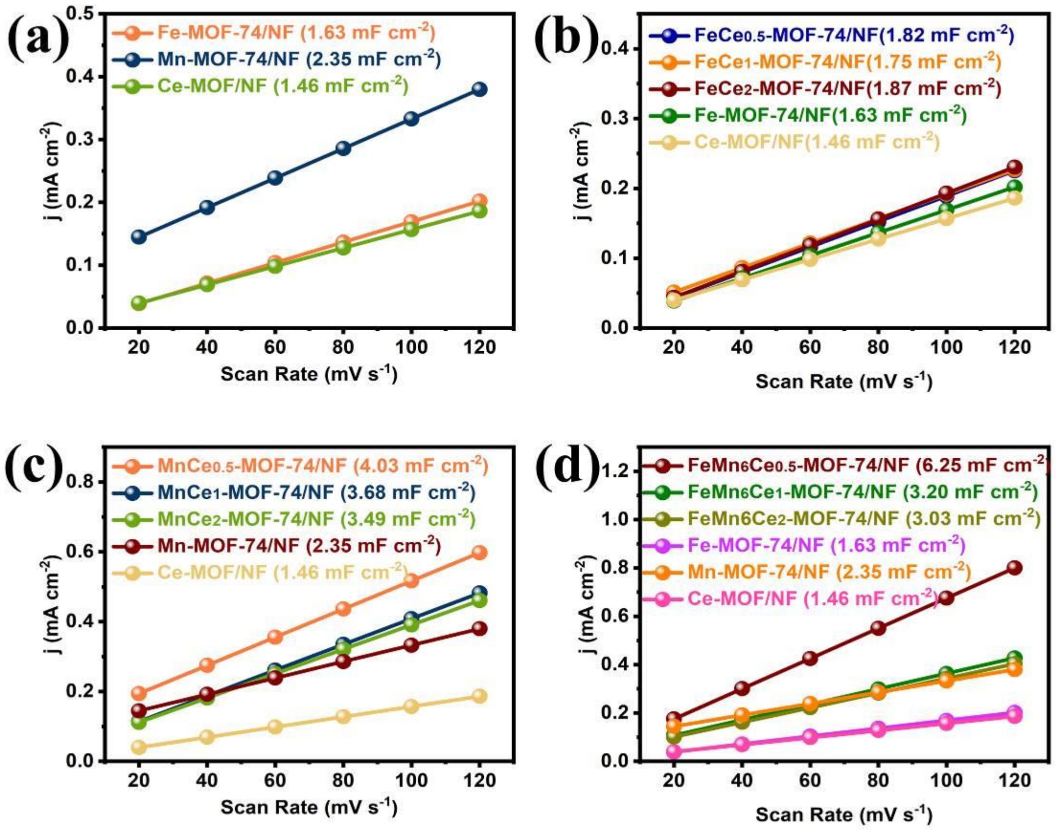

Fig. S14 C_{dl} data of Nyquist plots of (a) single metal-MOF-74; (b) FeCe-MOF-74 series; (c) MnCe-MOF-74 series and (d) (FeMnCe)-MOF-74 series.

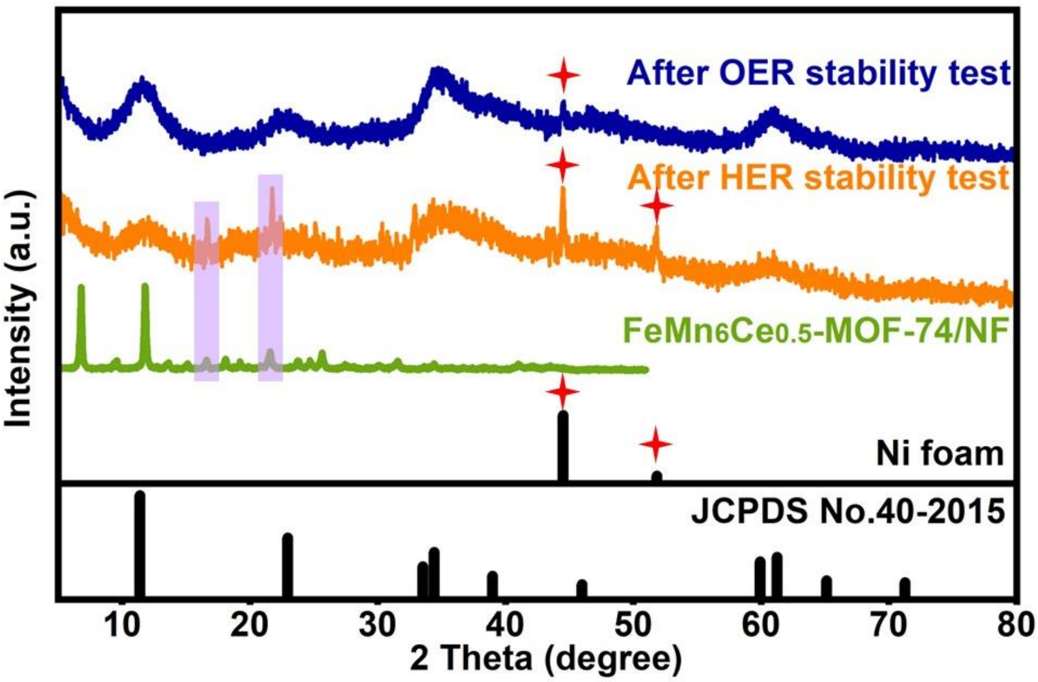

Fig. S15 XRD patterns of the $FeMn_6Ce_{0.5}$-MOF-74/NF after the OER and HER for 24 h electrolysis process.

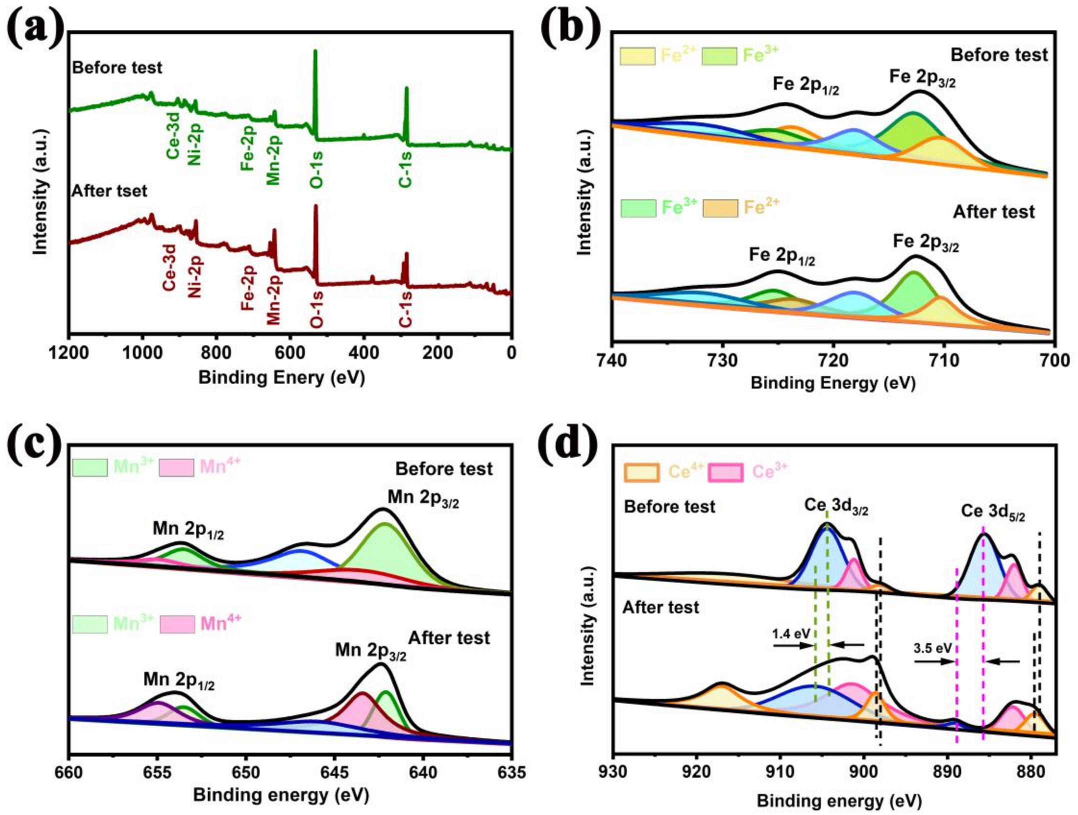

Fig. S16 (a) XPS survey spectrum for $FeMn_6Ce_{0.5}$-MOF-74/NF before and after OER stability test. XPS analyses of Fe 2p (b), Mn 2p (c) and Ce 3d (d) before and after OER stability test.

In Fig. S16, showed the high-resolution Fe 2p, Mn 2p, and Ce 3d XPS spectra for $FeMn_6Ce_{0.5}$-MOF-74/NF before and after the OER stability test. Fe 2p spectrum in $FeMn_6Ce_{0.5}$-MOF-74/NF shows two pairs of peaks 712.3 eV (Fe $2p_{3/2}$), 725.3 eV (Fe $2p_{1/2}$) for Fe^{3+} and 710.3 eV (Fe $2p_{3/2}$), 723.6 eV (Fe $2p_{1/2}$) for Fe^{2+}, and two satellite peaks 718.0 eV and 731.7 eV.[S1-3] In the high-resolution Mn 2p region of $FeMn_6Ce_{0.5}$-MOF-74/NF, two main peaks centered at 642.4 eV (Mn $2p_{3/2}$) and 653.5 eV (Mn $2p_{1/2}$) with one satellite peaks. It could be deconvoluted to four characteristic peaks at 641.4 eV and 653.0 eV could be assigned to Mn^{2+} and those at 653.7 eV with 642.9 eV correspond to the Mn^{3+} species.[S4-6] The binding energies 645.6eV satellite peaks also correspond to Mn^{2+}. Moreover, in the 3d Ce spectrum, the two peaks that appeared at 882.0 eV and 901.4 eV are assigned to $3d_{5/2}$ and $3d_{3/2}$ of Ce^{3+}, respectively. Then it had peaks at 898.1 eV, 915.8 eV, and 879.0 eV corresponding to Ce $3d_{3/2}$ and Ce $3d_{5/2}$ of Ce^{4+}. In addition, 885.6 eV and 904.4 eV were two satellite peaks.[S7-9]

Table S1. Content of four metal species in $FeMn_6Ce_{0.5}$-MOF-74、$FeMn_6Ce_1$-MOF-74 and $FeMn_6Ce_2$-MOF-74 by ICP-OES tests

	Mass%			Atom%		
	Fe	**Mn**	**Ce**	**Fe**	**Mn**	**Ce**
$FeMn_6Ce_{0.5}$	3.7	5.8	3.3	0.0661	0.1055	0.0235
$FeMn_6Ce_1$	2.9	4.7	3.6	0.0512	0.0861	0.0258
$FeMn_6Ce_2$	2.5	5.3	8.9	0.0450	0.0966	0.0639

Table S2. The comparison of the OER activities of $FeMn_6Ce_{0.5}$-MOF-74/NF and other recently reported MOF-based catalysts.

Catalyst	Overpotential (mV@mA cm^{-2})	Electrolyte	Ref
CoNi-MOF-74	300@100	0.1 M KOH	60
$Co_{0.6}Fe_{0.4}$-MOF-74	280@10	1.0 M KOH	46
Co_3O_4@MOF-74	285@50	1.0 M KOH	61
FeMn-MOF/NF(1:1)	290@50	1.0 M KOH	62
$Ni_{0.5}Co_{1.5}$- bpy(PyM)	256@10	1.0 M KOH	25
Br-Ni-MOF(A)	306@10	1.0 M KOH	20
NiFe(20Ni)-MOF/NFF	297@100	1.0 M KOH	63
Co_3Cu-Ni_2MOFs	288@10	1.0 M KOH	64
S/N-CMF@Fe_xCoyNi_{1-x-y}-MOF	296 @10	1.0 M KOH	11
Mn-MOF/NF	280@20	0.1 M KOH	30
FeCoNi MOF/NF	267@10	1.0 M KOH	65
CdFe-MOF	290@100	1.0 M KOH	66
$FeMn_6Ce_{0.5}$-MOF-74/NF	**281@100**	**1.0 M KOH**	**This work**

Reference

S1. W. Zhou, Z. Xue, Q. Liu, Y. Li, J. Hu and G. Li, *ChemSusChem*, 2020, **13**, 5647-5653.

S2. Q. Zha, M. Li, Z. Liu and Y. Ni, *ACS Sustainable Chem. Eng.*, 2020, **8**, 12025-12035.

S3. J. Xing, K. Guo, Z. Zou, M. Cai, J. Du and C. Xu, *Chem. Commun.,* 2018, **54**, 7046-7049.

S4. A. Goswami, D. Ghosh, D. Pradhan and K. Biradha, *ACS Appl. Mater. Interfaces,* 2022, **14,** 29722-29734.

S5. T. Tang, W. J. Jiang, S. Niu, N. Liu, H. Luo, Y. Y. Chen, S. F. Jin, F. Gao, L. J. Wan and J. S. Hu, *J. Am. Chem. Soc.,* 2017, **139**, 8320-8328.

S6. Y. Zhang, Z. Zeng and D. Ho, *Mater. Chem. Front.*, 2020, **4**, 1993-1999.

S7. P. Liu, Y. Lu, W. Ma, L. Ma, Q. Liu, X. Zhang and J. Guo, *Sustainable Energy Fuels*, 2019, **3**, 3344-3351.

S8. Y. Wang, S. Hao, X. Liu, Q. Wang, Z. Su, L. Lei and X. Zhang, *ACS Appl. Mater. Interfaces*, 2020, **12**, 37006-37012.

S9. M. Dinari, H. Allami and M. M. Momeni, *J. Electroanal. Chem.*, 2020, **877**, 114643.